Bound states in continuum: Quantum dots in a quantum well

Nikola Prodanović [a],[*], Vitomir Milanović [b], Zoran Ikonić [a], Dragan Indjin [a], Paul Harrison [a]

[a] *Institute of Microwaves and Photonics, School of Electronic and Electrical Engineering, University of Leeds, Woodhouse Lane, Leeds LS2 9JT, UK*
[b] *School of Electrical Engineering, University of Belgrade, Bulevar Kralja Aleksandra 73, 11000 Belgrade, Serbia*

A B S T R A C T

We report on the existence of a bound state in the continuum (BIC) of quantum rods (QR). QRs are novel elongated InGaAs quantum dot nanostructures embedded in the shallower InGaAs quantum well. BIC appears as an excited confined dot state and energetically above the bottom of a well subband continuum. We prove that high height-to-diameter QR aspect ratio and the presence of a quantum well are indispensable conditions for accommodating the BIC. QRs are unique semiconductor nanostructures, exhibiting this mathematical curiosity predicted 83 years ago by Wigner and von Neumann.

© 2013 Elsevier B.V. All rights reserved.

1. Introduction

Semiconductor quantum dots exhibit full 3D confinement for carriers, giving a few bound integrable states with a discrete spectrum below the barrier, and free non-integrable states with continuum spectrum above the barrier. Quantum dots are often referred to as "artificial atoms" due to their discrete part of spectrum and discrete optical resonances arising from transitions between bound orbital states. Both atoms and quantum dots can be ionized, when electrons gain sufficient energy to escape the binding potential, and subsequently occupy free states – in vacuum in the case of atoms or bulk in the case of quantum dots.

However, boundedness and discreteness of an orbital state in quantum dots do not come necessarily together. We show in this Letter that novel semiconductor nanostructures, so called quantum rods, exhibit bound excited state with an energy embedded in the continuum of other free electronic states, above the ionization threshold. This is a so called bound state in continuum (BIC). There are various types of BIC reported since the foundation of quantum mechanics, but none of them were reported for atomic or condensed matter systems. In what follows, we state only a few. The first prediction originates back to 1929 when von Neumann and Wigner showed such a possibility by mathematical construction of a bounded potential accommodating a BIC [1]. This issue was revitalized by Stillinger and Herick [2] pointing out, 46 years later, that a BIC could occur in some specific molecular systems. The first artificial semiconductor nanostructure accommodating the bound state above ionization threshold, was reported in Ref. [3]. This

bound state was argued to be a consequence of Bragg reflection due to the superlattice. Even though above the barrier, this state wasn't surrounded by a continuum of states and it was strictly speaking a quasi-bound state with free motion in the lateral direction. Some theoretical proposals and proofs for the BIC existence were reported for more complex quantum mechanical systems. For example, coupled system of electrons and nuclei in molecules [4] was considered. BIC, as an quantum mechanical interference effect can occur in various abstract models. Some examples of theoretical abstract systems that support BIC were reported in Refs. [5–10]. Experimentally, only photonic crystal systems with the BIC were reported [11,12]. A theoretical design of one-dimensional photonic heterostructure, supporting the BIC was provided in Ref. [13].

In what follows, we briefly describe the geometrical and compositional properties of quantum rods, and based on that we provide proof for BIC existence. The type of BIC which occurs in quantum rods is somewhat different from the majority of BICs reported in the literature. The most similar system supporting the BIC was reported by Robnik et al. [14], and one could say that the BIC reported here represents the 3D generalization of the 2D potential theoretically constructed in [14]. The rest of the Letter is dedicated to the discussion of possible interesting features arising from BIC existence, together with available experimental data and concluding remarks.
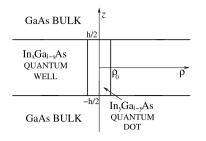
2. Quantum rods

Quantum rods are elongated InGaAs quantum dots embedded in a InGaAs quantum well sandwiched by two GaAs bulk regions. Details of the QR fabrication can be found in Refs. [15–17]. A simplified model for geometric and compositional properties of these

* Corresponding author. Tel.: +44 7587029902.
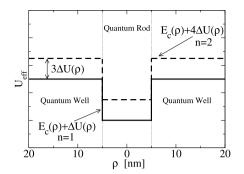*E-mail address:* elnpr@leeds.ac.uk (N. Prodanović).

Fig. 1. Simplified geometric model of a quantum rod. Cylindrical symmetry is assumed, so the entire structure can be depicted within the z–ρ plane. Indium content of the dot region is larger than in the well region, i.e. $x < y$.

nanostructures is presented in Fig. 1. This structure consists of GaAs/InGaAs quantum well of width h over the region between $-h/2$ and $h/2$. The quantum dot is positioned within the quantum well so that the bulk region is above and below the dot in the z-direction and the quantum well is surrounding the rod in the radial direction. The entire structure is optically active giving the combined features of dot, well and the bulk as it is obvious from PL measurements [16,18]. The height of the rod and the width of the surrounding well are the same. This simplified model assumes that entire structure is cylindrically symmetric, even though such strict symmetry hasn't been reported. However, the general conclusions that follow do not depend on the exact shape of the rod basis. Therefore, we choose the circular shape of the basis in order to simplify theoretical consideration. The quantum rod has higher In content then the surrounding quantum well which makes the dot energetically deeper than the surrounding well.

3. Bound state in the continuum

One can naively expect that the quantum rod would accommodate bound states only below the quantum well barrier in the radial direction. However, due to bulk confinement in the z-direction, bound states could also appear with energies above the well barrier where also well continuum states are present giving the BIC. Such a situation resembles the one from Ref. [3] where a bound state occurs above the barrier of a superlattice, but it isn't surrounded by continuum states because the state itself is an impurity state in the superlattice, spaced from the continuum superlattice bands. Also, such a BIC is strictly speaking a quasi-bound state. We prove that in the case of a quantum rod, such state above the barrier is indeed surrounded by the continuum and is indeed bound for a wide range of parameter space.

Existence of the BIC in quantum rods is purely due to the interplay of the combined well and dot confinement. In order to prove this statement, consider the idealized quantum rod structure presented in Fig. 1. The quantum rod is considered isolated from the other quantum rods. We assume cylindrical symmetry of the entire structure, and the value of the embedding bulk barrier is set to infinity. The assumption of infinitely high bulk walls does not affect the general conclusion since the same conclusion follows from the full 8-band $\mathbf{k} \cdot \mathbf{p}$ model where the values for all barriers in the structure were taken with precise offsets and included strain effects. Now it becomes clear that this simplified model of realistic quantum rods presents the 3D generalization of the 2D potential constructed by Robnik et al. [14] in order to obtain the BIC, with the quantum well as escaping channel. However, it was pointed out in the same reference that existence of BIC in such potential is sensitive to perturbation, especially the one which might break the parallel geometrical shape of escaping channel. That shouldn't be a problem in this case, since the existence of quality quantum well seems very eminent, and the walls of quantum well escaping channel can be considered parallel to the infinity.

Fig. 2. Illustration of the energy span where a BIC can occur. The effective potential U_{eff} for the remaining one-dimensional radial eigenproblem is given for $l = 0$ and $n = 1, 2$. For $n = 1$ continuum states or quasi-bound well states occur for $E > U_b + \Delta U$. For $n = 2$ bound states might occur for $E < U_b + 4\Delta U$, whereas continuum states occur for $E > U_b + 4\Delta U$. Therefore the excited bound state in the well quasi-band continuum might occur for energies in the range $U_b + \hbar^2 \pi^2 / 2m_w h^2 < E < U_b + 2\hbar^2 \pi^2 / m_w h^2$.

In this simple model we solve one spinless electron single-band envelope function equation in polar coordinates:

$$\left(\frac{\hbar^2}{2} \nabla \frac{1}{m_e(\mathbf{r})} \nabla + E_c(\rho) + E_c^z(z) \right) \Psi(\mathbf{r}) = E \Psi(\mathbf{r}) \qquad (1)$$

where

$$E_c(\rho) = \begin{cases} 0 & \text{for } \rho < \rho_0 \\ U_b & \text{for } \rho > \rho_0 \end{cases}$$

and

$$E_c^z(z) = \begin{cases} 0 & \text{for } -\frac{h}{2} < z < \frac{h}{2} \\ \infty & \text{for } z < -\frac{h}{2} \text{ or } z > \frac{h}{2} \end{cases}$$

Values of the effective mass $m_e(\mathbf{r})$ are m_d and m_w in the dot and the well respectively. In the bulk, where the value of the potential is set to infinity, the value of the effective mass is unnecessary. The potential offset between dot and the well region is U_b. Parameters ρ_0 and h are the radius and the height of the QR. Due to infinite bulk barrier and cylindrical symmetry, one can separate the variables of the wavefunction $\Psi(\mathbf{r}) = \Phi(\phi)Z(z)R(\rho)$. Furthermore, the solutions for $\Phi(\phi)$ and $Z(z)$ are $\Phi_l(\phi) = \frac{1}{\sqrt{2\pi}} e^{il\phi}$ and $Z_n(z) = \sqrt{\frac{2}{h}} \sin(\frac{n\pi}{h}(z + \frac{h}{2}))$ where we introduce good quantum numbers l and n, integer and positive integers respectively. The remaining Schrödinger-like equation in the radial direction reads:

$$-\frac{\hbar^2}{2} \frac{1}{\rho} \frac{\mathrm{d}}{\mathrm{d}\rho} \frac{\rho}{m_e(\rho)} \frac{\mathrm{d}}{\mathrm{d}\rho} R_{nl}(\rho)$$
$$+ \left(E_c(\rho) - E + \frac{\hbar^2}{2m_e(\rho)} \left(\frac{n^2\pi^2}{h^2} + \frac{l^2}{\rho^2} \right) \right) R_{nl}(\rho) = 0 \qquad (2)$$

We provide the full solution to Eq. (2) in Appendix A. In order to maintain the simplicity, we will demonstrate the existence of the BIC by considering only the case with $l = 0$ and $n = 1, 2$.

The effective potential for the last eigenproblem in Eq. 2 is the expression given in brackets. The effective potential for $n = 1$ is $U_{\text{eff}}(\rho) = E_c(\rho) + \Delta U(\rho)$, where $\Delta U(\rho) = \hbar^2 \pi^2 / 2m_e(\rho)h^2$ and for $n = 2$ it is $U_{\text{eff}}(\rho) = E_c(\rho) + 4\Delta U(\rho)$. The effective potential for $l = 0$ and $n = 1, 2$ is given in Fig. 2. Note that the effective mass depends only on the radial coordinate since the value of the effective mass in bulk is irrelevant due to infinite potential.

For $n = 1$ continuum states or quasi-bound well states occur for $E > U_b + \hbar^2 \pi^2 / 2m_w h^2$. For $n = 2$ bound states might occur for $E < U_b + \hbar^2 2\pi^2 / m_w h^2$, whereas continuum states occur for $E > U_b + 2\hbar^2 \pi^2 / m_w h^2$. Therefore, the excited bound state for $n = 2$

in the well quasi-band continuum for $n = 1$ (above the ionization threshold) might occur at an energy between $U_b + \hbar^2\pi^2/2m_w h^2 < E < U_b + 2\hbar^2\pi^2/m_w h^2$. Note that the first bound states for $l = 0$, $n = 1, 2$ are so called s-like and p-like states as often referred to in literature. We give the numerical example of this p-like BIC in the next section.

4. Numerical results

In our previous work [19] we have calculated detailed electronic structure of the realistic quantum rods grown in [16] by using the 8-band $\boldsymbol{k} \cdot \boldsymbol{p}$ method with strain effects included. In this Letter we will use one-band model derived in previous chapter in order to demonstrate the existence of BIC and 8-band results will be used as a supporting reference.

For the fabricated rods reported in Ref. [16], the In content in the dot and the well is typically 0.45 and 0.16, respectively, and their radius was estimated to be around 5 nm. For such a structure we have extracted the value of dot-well band offset $U_b = 120$ meV, using the full 8 band $\boldsymbol{k} \cdot \boldsymbol{p}$ model with strain effects included [19]. The height of the rods from Ref. [16] is in the range 10–40 nm.

In the following, all energies are referenced to the bottom of the conduction band of the rod material. For the typical rod height of 10 nm, the continuum for $n = 1$ starts at 182 meV, and the p-like bound state for $n = 2$ is below the $n = 2$ continuum, starting at 356 meV. The splitting between s-like ground state and p-like first excited state (which is the BIC) is 200 meV. For the same rod, but with 15 nm height, we find 2 additional bound states, for $l = 0$ and $n = 3$ and 4, which are also embedded in the continuum. There are no discrete states solutions for $l > 0$. By increasing the rod height we generally get more bound states in the continuum, since new bound states with higher values of n appear. However, the energy of all bound states gets lower with increasing the quantum rod height [19], and consequently bound states with the lowest n might sink under the $n = 1$ continuum, ceasing to be BIC. Also, by increasing the rod radius, additional states may appear with higher value of quantum number l. These states may also become BIC.

Energy diagram of a 10 nm tall rod calculated by 8-band model is presented in Ref. [19]. Energy diagram clearly show the existence of the BIC. The higher the rod, the higher is the excited dot state embedded in continuum. For the 10 nm tall rod, the splitting between ground state and the bound state in the continuum is 150 meV. Higher value of s–p splitting is due to infinite potential barrier in growth direction which was realistically taken to be finite in 8-band model. In this work we used one-band model with infinite barriers as a default model in order to get insight in physics arguments of the BIC existence.

Therefore, we proved the existence of the bound state in continuum as a sole consequence of combined well-dot confinement, and for a wide range of structure parameters, especially the adjustible rod height.

5. Discussion

The above consideration shows that BIC occurs for higher values of the quantum number n, i.e. BIC has at least one node in the growth direction. The quantum rod must be sufficiently tall in order to support at least two bound states (s-like and p-like) localized in the dot due to the growth confinement, i.e. with quantum number $n > 0$. With increasing quantum number n, the effective potential $U_{\text{eff}}(\rho) = E_c(\rho) + \Delta U(\rho)$ might become a barrier instead of a well, since $m_d < m_w$. Therefore, the upper bound on a value of n for which BIC exists is imposed $n < \frac{h}{\pi}\sqrt{\frac{U_b}{\hbar^2}\frac{m_w m_d}{m_w - m_d}}$ where m_w and m_d are effective masses of the well and the dot respectively.

We also conclude that confinement in the growth direction has to be stronger than the confinement in the radial direction caused by the shallower well. At the same time, well subbands may have energies lower than the bulk barrier, opening the possibility that their energy equals the energy of the excited bound state of the dot.

In similar nanostructures, quantum dots in a quantum well (DWELL), this effect does not exist. Conventional quantum dots have very low height to diameter aspect ratio and an excited bound state is guided by the radial confinement, i.e. the excited bound states have nodes in the radial direction and there is no bound state with nodes in the growth direction. Therefore, energy of such an excited state cannot be higher than the well barrier in the radial direction. One thus concludes that quantum rods are unique semiconductor nanostructures with 3D bound state in continuum as a consequence of their distinct features: high value of height-to-diameter aspect ratio and existence of the shallower surrounding well.

We have previously shown in Ref. [19] that only the growth-polarized light can excite an electron from the ground dot state in the conduction band to the first excited dot state which can be set to be BIC for particular heights of the rod. This is so called s–p-like optical transition. Such a transition is expected to be a single broadened line. We argue that homogeneous broadening is expected to be high due to effective interference of the continuum with the bound state via phonons. We also argue that asymmetrical lineshape of such optical resonance should be expected, also a consequence of interference of the continuum and p-like bound state along the resonant s–p transition. However, we do not expect that asymmetrical lineshape is observable due to high broadening and other resonances.

Intraband resonances of quantum rods were investigated in Ref. [17], where the rods were charged with several electrons, enough to completely fill the 3D confined states below the well barrier. Authors then used growth-polarized radiation to excite electrons, and they recognized a clear difference between well and dot resonances. The leading rod resonance comes from transition from excited and fully charged rod states to unoccupied states higher in the conduction band. However, authors in Ref. [17] argued that electron–electron interaction in fully charged rods shifts the bound electronic states to higher energies. Detailed theoretical examination of that situation is required due to electron–electron interaction which is responsible for perforation of the 2D electron gas, i.e. continuum. Nevertheless, the short lifetime of the BIC via fast scattering into the well subband was indicated in Ref. [17]. It is intuitively clear that such fast scattering occurs due to the availability of the continuum of free states around the energy of the BIC.

Altogether, one can conclude that carriers from the bound quantum rod state can be efficiently scattered into the continuum of the well by strong optical resonance due to ground state-BIC transition and coupling between the BIC and surrounding continuum. The similar effect, where strong optical resonance can trigger ionization from bound-like state to continuum state where carriers can freely move was explained in Ref. [20] for the case of 1D supercrystal formed of the vertically stacked self-assembled quantum dots. Specifically, first supercrystal miniband occurs in the barrier gap and second one in the conduction band. Optical transitions between these two minibands are strong since those minibands were formed of s-like and p-like states respectively. Therefore, this structure, if constructed as solar cell, exhibits increased efficiency due to strong transitions between first miniband burried in the barrier gap and second miniband buried within the conduction band continuum. In addition, strong optical transitions between below-the-barrier and above-the-barrier bound states were observed experimentally in Ref. [3] in a Bragg-confined quantum well structure.
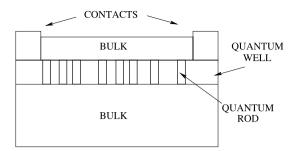
Fig. 3. Illustration of the polarization-independent terahertz photodetector. In this geometry, the electric field due to the bias on contacts is in the lateral direction.

These exotic optical properties of the BIC could allow experimental observation of the BIC and associated effects. The simplest version of such an experiment is based on doped structures with up to one electron per rod. In such a case, intraband optical transitions at low temperatures are limited to the transitions from the ground state. One could measure the absorption of far-infrared light in such doped quantum rods at low temperatures for two linearly polarized directions of incident light. We have also shown in Ref. [19] that radially polarized light can excite the electron from the same ground dot state to the first well subband. This transition is not expected to be a single broadened line due to the continuum of the well subband, but resonances are expected to start at an energy corresponding to the bottom of the first subband of the well. If these resonances for the radially polarized radiation were at lower energy than the first resonance for the growth-polarized radiation, this would present a clear evidence that the excited bound state has a higher energy than the minimum of the well subband, proving the existence of BIC.

Finally, we will briefly discuss a possible application of this effect. If an electron, excited into the BIC, efficiently scatters into the well subband, as indicated in Ref. [17], then a radially directed electric field can be used for efficient transport of carriers in the lateral direction. Strong optical resonance for the growth-polarized radiation is due to bound-to-bound transition and efficient transport can occur via radially free state channels around the excited bound state. On the other hand, for radially polarized incident radiation, carriers are excited directly into the well subband [19], from which they can be easily extracted by a lateral electric field. Therefore, strong resonance and efficient transport can be obtained for either polarization of the incident light, paving the way for polarization-independent terahertz detector. Such a detector is schematically depicted in Fig. 3. Contacts are positioned so to provide a lateral electric field. Upon absorption of the incident radiation the electron concentration in the well increases and leads to a photocurrent. However, strong reverse process was indicated in Ref. [21] that carriers in the conduction band of the well and bulk also efficiently scatter into the rod which can degrade the effect of detection. Therefore, this proposition for the efficient photodetector utilizing bound-to-BIC transition still needs to be carefully examined.

6. Conclusion

In summary, we proved that quantum rods can accommodate the excited normalizable state, energetically embedded in the continuum of the subband of the quantum well embedding it, where the electrons can be ionized into. We proved that existence of such states is entirely due to the interplay of two different types of confinement, namely the dot 3D confinement and the well confinement in the growth direction. We indicated that QRs are unique structures with this exotic mathematical property. As recently realized structures, quantum rods have not been extensively studied

experimentally, and we expect that interesting dynamical features due to the combined properties of bound and free states could arise.

Acknowledgements

Appendix A. Full solution to the model

In this appendix we provide the full solution to the radial equation (2). It can be rewritten as

$$\rho^2 \frac{d^2 R(\rho)}{d\rho^2} + \rho \frac{dR(\rho)}{d\rho} + \left((k_{d/w}^n)^2 \rho^2 - l^2 \right) R(\rho) = 0 \qquad (A.1)$$

where the radial wavenumber depends on quantum number n only and is defined as

$$\left(k_{d/w}^n \right)^2 = \frac{2m_{d/w}}{\hbar^2} \left[E - E_{c,d/w} - \frac{\hbar^2 n^2 \pi^2}{2m_{d/w} h^2} \right] \qquad (A.2)$$

Subscripts d and w refer to the dot and well domain, respectively. All material parameters are constant within each of these regions. For a fixed n, the wavenumber squared for the dot region $(k_d^n)^2$ is positive in the range of energies $E > \frac{\hbar^2 n^2 \pi^2}{2m_d h^2}$. However, the wavenumber squared for the well region $(k_w^n)^2$ is negative in energy interval $E < U_b + \frac{\hbar^2 n^2 \pi^2}{2m_w h^2}$.

Therefore, the solution for an energy in the interval $\frac{\hbar^2 n^2 \pi^2}{2m_d h^2} < E < U_b + \frac{\hbar^2 n^2 \pi^2}{2m_w h^2}$ reads

$$R_{nl}(\rho) = \begin{cases} C_1 J_l(k_d^n \rho) & \text{for } \rho < \rho_0 \\ C_2 K_l(\kappa_w^n \rho) & \text{for } \rho > \rho_0 \end{cases} \qquad (A.3)$$

where we used the standard Bessel function notation and introduced $(\kappa_{w/d}^n)^2 = -(k_{w/d}^n)^2$ which is positive real number for the considered energy interval. The Bessel function of the second kind Y_l and modified Bessel function of the first kind I_l are absent from the solution due to their divergent behavior in corresponding domains. Boundary conditions at $\rho = \rho_0$ are the continuity of radial wavefunction and continuity of its derivative divided by effective mass, and lead to homogeneous system of linear equations in C_1 and C_2 which has a solution if

$$\frac{\kappa_w^n}{m_w} J_l(\rho_0 k_d^n) \frac{d}{d\rho} \left(K_l(\rho_0 \kappa_w^n) \right) = \frac{k_d^n}{m_d} K_l(\rho_0 \kappa_d^n) \frac{d}{d\rho} \left(J_l(\rho_0 k_d^n) \right) \quad (A.4)$$

By solving this transcendent equation one obtains the discrete energy spectrum for fixed n and l and those solutions are numbered with index j. Eq. (A.4) has to be solved in the energy range $\frac{\hbar^2 n^2 \pi^2}{2m_d h^2} < E < U_b + \frac{\hbar^2 n^2 \pi^2}{2m_w h^2}$, but further narrowing of this range exists for $l \neq 0$. Taking into account the condition that energies of discrete levels have to be above the minima of effective potential one can show that narrowed energy range for solving Eq. (A.4) is $\frac{\hbar^2}{2m_d} \left(\frac{n^2 \pi^2}{h^2} + \frac{l^2}{\rho_0^2} \right) < E < U_b + \frac{\hbar^2 n^2 \pi^2}{2m_w h^2}$.

Each discrete energy defines the radial wavenumbers $k_{w/d}^{nj}$ and $\kappa_{w/d}^{nj}$ which do not depend explicitly on l (only implicitly,

via the solutions for discrete spectrum). The corresponding radial wavefunctions are

$$R_{nlj}(\rho) = \begin{cases} C_1 J_l(k_d^{nj}\rho) & \text{for } \rho < \rho_0 \\ C_1 \frac{J_l(k_d^{nj}\rho_0)}{K_l(\kappa_w^{nj}\rho_0)} K_l(\kappa_w^{nj}\rho) & \text{for } \rho > \rho_0 \end{cases} \quad (A.5)$$

where the C_1 is determined by normalization.

For the remaining range of energies, i.e. $E > U_b + \frac{\hbar^2 n^2 \pi^2}{2m_w h^2}$ the spectrum is continual and for each energy the corresponding radial wavefunction is

$$R_{nlE}(\rho) = \begin{cases} C_1 J_l(k_d^n\rho) & \text{for } \rho < \rho_0 \\ C_2 J_l(k_w^n\rho) + C_3 Y_l(k_w^n\rho) & \text{for } \rho > \rho_0 \end{cases} \quad (A.6)$$

By using the same boundary and normalization condition one can obtain the constants C_1, C_2 and C_3. There are infinitely many continuum states for any energy counted by quantum number l, in contrast to discrete part of the spectrum where boundary conditions do not allow solutions to exist for values of quantum number l higher than some critical value. Such upper bound to the quantum number l depends also on quantum number n. For increasing value of n, the upper bound of l decreases and eventually there will be no discrete states for some critical value of quantum number n.

Consider now the general case of discrete states with quantum numbers $n = q_n$ and $l = q_l$. Such states can occur in the energy range $\frac{\hbar^2}{2m_d}(\frac{q_n^2\pi^2}{h^2} + \frac{q_l^2}{\rho_0^2}) < E < U_b + \frac{\hbar^2 q_n^2 \pi^2}{2m_w h^2}$. (It is implicitly assumed that q_n and q_l are small enough so $\frac{\hbar^2}{2m_d}(\frac{q_n^2\pi^2}{h^2} + \frac{q_l^2}{\rho_0^2}) < U_b + \frac{\hbar^2 q_n^2 \pi^2}{2m_w h^2}$.) We want to find the conditions for which the continuum with quantum number $n = p$ can embed the given bound state. The continuum with quantum number $n = p$ exists for energies $E > U_b + \frac{\hbar^2 p^2 \pi^2}{2m_w h^2}$. Therefore, if $U_b + \frac{\hbar^2 p^2 \pi^2}{2m_w h^2} < \frac{\hbar^2}{2m_d}(\frac{q_n^2\pi^2}{h^2} + \frac{q_l^2}{\rho_0^2})$, then a bound state with quantum numbers $n = q_n$ and $l = q_l$ can occur in the continuum of quantum number p in the range of energies $\frac{\hbar^2}{2m_d}(\frac{q_n^2\pi^2}{h^2} + \frac{q_l^2}{\rho_0^2}) < E < U_b + \frac{\hbar^2 q_n^2 \pi^2}{2m_w h^2}$.

On the other hand, if $U_b + \frac{\hbar^2 p^2 \pi^2}{2m_w h^2} > \frac{\hbar^2}{2m_d}(\frac{q_n^2\pi^2}{h^2} + \frac{q_l^2}{\rho_0^2})$ then bound state in the continuum occurs for energies satisfying $U_b + \frac{\hbar^2 p^2 \pi^2}{2m_w h^2} < E < U_b + \frac{\hbar^2 q_n^2 \pi^2}{2m_w h^2}$.

References

[1] J. von Neumann, E. Wigner, Zeitschrift für Physik 30 (1929) 465.
[2] F.H. Stillinger, D.R. Herrick, Physical Review A 11 (1975) 446.
[3] F. Capasso, C. Sirtori, J. Faist, D.L. Sivco, S.G. Chu, A.Y. Cho, Nature 358 (1992) 565.
[4] L.S. Cederbaum, R.S. Friedman, V.M. Ryaboy, N. Moiseyev, Physical Review Letters 90 (2003) 013001.
[5] H. Nakamura, N. Hatano, S. Garmon, T. Petrosky, Physical Review Letters 99 (2007) 210404.
[6] N. Moiseyev, Physical Review Letters 102 (2009) 167404.
[7] J.S. Petrovic, V. Milanovic, Z. Ikonic, Physics Letters A 300 (2002) 595.
[8] A.F. Sadreev, E.N. Bulgakov, I. Rotter, Physical Review B 73 (2006) 235342.
[9] M.I. Molina, A.E. Miroshnichenko, Y.S. Kivshar, Physical Review Letters 108 (2012) 070401.
[10] W. Hsueh, C. Chen, C. Chang, Physics Letters A 374 (2010) 4804.
[11] D.C. Marinica, A.G. Borisov, S.V. Shabanov, Physical Review Letters 100 (2008) 183902.
[12] Y. Plotnik, O. Peleg, F. Dreisow, M. Heinrich, S. Nolte, A. Szameit, M. Segev, Physical Review Letters 107 (2011) 183901.
[13] N. Prodanovic, V. Milanovic, J. Radovanovic, Journal of Physics A – Mathematical and Theoretical 42 (2009) 415304.
[14] M. Robnik, Journal of Physics A – Mathematical and General 19 (1986) 3845.
[15] P. Ridha, L. Li, A. Fiore, G. Patriarche, M. Mexis, P.M. Smowton, Applied Physics Letters 91 (2007) 191123.
[16] L. Li, G. Patriarche, N. Chauvin, P. Ridha, M. Rossetti, J. Andrzejewski, G. Sek, J. Misiewicz, A. Fiore, IEEE Journal of Selected Topics in Quantum Electronics 14 (2008) 1204.
[17] C.M. Morris, D. Stehr, H. Kim, T.-A. Truong, C. Pryor, P.M. Petroff, M.S. Sherwin, Nano Letters 12 (2012) 1115.
[18] R. Nedzinskas, B. Cechavicius, J. Kavaliauskas, V. Karpus, G. Valusis, L. Li, S. Khanna, E. Linfield, Nanoscale Research Letters 7 (2012) 609.
[19] N. Prodanović, N. Vukmirović, D. Indjin, Z. Ikonić, P. Harrison, Journal of Applied Physics 111 (2012) 073110.
[20] S. Tomić, Physical Review B 82 (2010) 195321.
[21] D. Stehr, C.M. Morris, D. Talbayev, M. Wagner, H.C. Kim, A.J. Taylor, H. Schneider, P.M. Petroff, M.S. Sherwin, Applied Physics Letters 95 (2009) 251105.